4.2 Beamline Engineering

4.2.1 Introduction

The objective of the beamline engineering effort is to design and build all the beamline FE components and to develop standard beamline components that would be of use to all APS CATs. Towards this objective, the team is built around the following expertise:

- knowledge of heat transfer engineering to handle high heat flux from IDs on various mechanical components of the beamline FEs (described in Chapter 2) and beamlines,
- fabrication of components using modern composite materials with the development of suitable bonding, brazing, and welding technologies, and
- precision engineering required in the design of support stages and manipulators for standard beamline components and optics.

The design and construction of these components have now been completed, and many of the beamline FEs and standard components are now installed. The details of this work can be found in various publications (Kuzay, 1993; Shu & Kuzay, 1994; Shu et al., 1992a; Shu et al., 1995).

During the past year, major effort has been devoted to evaluation of the performance of these mechanical components of the beamlines. In addition, we have conducted special experiments to test the performance limits of some of the critical elements of both the beamline FEs located behind the shield wall of the storage ring and the user beamlines installed on the experiment hall floor. The performance to date of some of these components and the ongoing R&D in support of the APS operations are summarized here.

Unless otherwise noted, the material presented here describes only the ID beamlines, as their designs are the most challenging and have the most stringent thermo-structural specifications.

4.2.2 Performance Review of the Important FE and Beamline Components

Vacuum Breach Tests in APS Beamline FEs

Measurement of the propagation of a pressure front under simulated FE vacuum-breach conditions has shown that the engineering of the apertures in the beamline FEs provides adequate vacuum delay to protect the storage-ring vacuum. The data for the ID beamline FEs were taken on the ID FE prototype (1:1 scale) (Liu et al., 1995); while the data for the BM beamline FEs were collected on 3-BM during operations.

In performing the vacuum-breach tests on the FE prototype, the simulation represented an equivalent of a 6 mm hole to the atmosphere in a 1-mm-thick window. Four ion gauges (IG1-IG4) were placed in the FE for measurement (see Fig. 4.22). Under such a severe vacuum breach, the pressure wave took 48 ms to reach IG1, 80 ms to IG2, and 110 ms to IG3 (Fig. 4.22a). Because the fast valve closed in

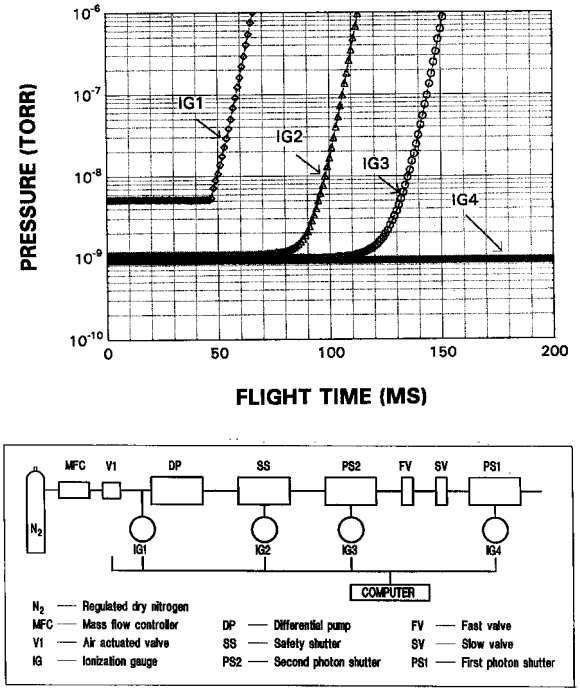

Fig. 4.22 ID FE vacuum-breach tests. (a) Time (in ms) for the pressure wave to reach the ion gauges. (b) Schematic of the location of the ion gauges (IG1-IG4).

6.7 ms, IG4 never experienced the pressure wave. Thus even with a large vacuum breach in a typical ID beamline, the FE has up to 50 ms delay time for proper closure of the vacuum valves to isolate the strickened FE from the storage-ring vacuum.

To date the only *in situ* FE vacuum-breach incident under real user beam operation conditions occurred on beamline 5-ID, which had a windowless configuration. As the result of a miscalculated beam steering request, the undulator radiation beam struck a bellows, which caused substantial outgassing and damage to the bellows. The resulting deterioration in the vacuum was sensed by the cold cathode gauge, which initiated proper EPS actions by closing the FE valves and isolating the FE. The FE recovered normally through subsequent pumping after the damaged bellows were replaced.

In situ vacuum-breach tests on the 3-BM FE were conducted in a fashion similar to those done on the ID FE prototype. To summarize, in the worst-case leak tests, a shock wave was generated by bleeding nitrogen into the FE at 50 psi for 3 seconds. The ion gauge by the safety shutter registered a 60 ms time delay, and the ion gauge by the first photon shutter (PS1) registered 120 ms delay time (vacuum valve closure was disabled). The measured vacuum delays are certainly long enough to activate the FE vacuum valves and in turn protect the vacuum conditions in the storage ring.

Photon shutter tests

The ID FE components have been designed to handle radiation beams from 2.4-m-long undulators when the storage ring is operated with a maximum of 100 mA of particle beam. In the FE, the most challenging components to design are the photon shutters. A series of tests were arranged to assess the performance limits of the user-operated photon shutter, PS2, at highest available stored beam currents. Because the maximum stored beam current is 100 mA during current operations, to simulate higher current operations, the incident angle of undulator beam with respect to the PS2 surface was increased to deliver higher heat flux on the shutter blade.

The beam defining mask associated with the windowless configuration of the FE allowed a full 5.3 kW of power from the undulator (gap of 11 mm and stored beam current of 100 mA) to impinge on the photon shutter during these tests. In order to increase the heat flux on the

shutter blade (located at 26 m from the source in this experiment), the blade was tilted to 6.75° with respect to the undulator beam. This generated a measured power of 4.3 kW at 100 mA or a maximum heat flux density of 27.5 W/mm^2 on the shutter surface.

The maximum temperature registered on the blade at a depth of 2 mm and approximately at the center of the beam footprint was about 340°C. While on the sides of the blade, temperatures of 90 and 70°C were measured. The measured 340°C inside the shutter blade corresponds to a 460°C surface temperature. The maximum measured flow enthalpy, as shown in Fig. 4.23, indicates that during the tests the power absorbed by the shutter is 4.1 kW at 11 mm gap and at 97 mA current (or 4.3 kW at 100 mA). This represents about 70% of the 5.3 kW full power from the beam at 11 mm gap and at 100 mA. These measurements agree closely with the pretest analysis using a finite element analysis code (ANSYS).

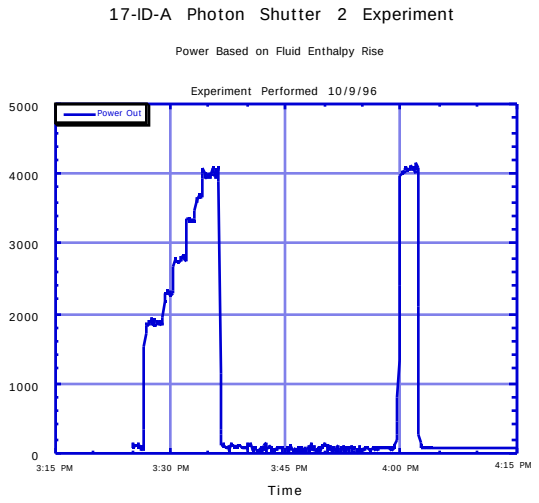

Fig. 4.23 Power absorbed by PS2 based on fluid enthalpy rise.

It is interesting to evaluate the performance of PS2 under its normal operational conditions, viz., its location at 20.1 m with a inclination angle of 2°. The power density handled in this configuration is about 13 W/mm^2, which is well below the maximum power handled in the tests at 27.5 W/mm^2.

The maximum current limit for the operation of PS2 can also be extrapolated from these studies. Figure 4.24 shows that the experimentally deduced 460°C surface temperature is reached at about 190 mA beam current at 11 mm gap and with PS2 located at 20.1 m from the source. The analysis showed that the coolant wall had reached 210°C, which would

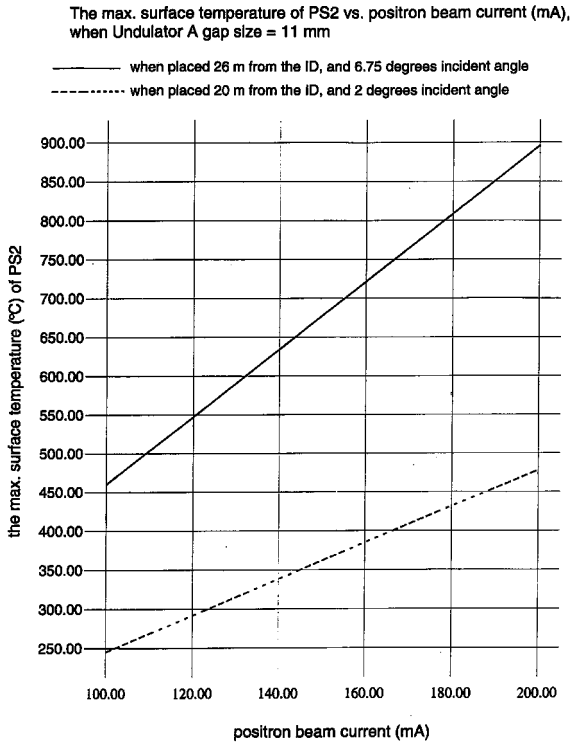

Fig. 4.24 Maximum surface temperature of PS2 versus positron beam current (with undulator A gap size = 11 mm). Solid line - PS2 is 26 m from the ID at an incident angle of 6.75°. Dotted line - PS2 is 20 m from the ID at an incident angle of 2°.

induce severe boiling. The shutter surface and/or the Glidcop/OFHC copper interface are most likely to experience fatigue under these operating conditions because of extremely high localized thermal stresses. The shutter can tolerate such conditions on a transient or infrequent basis but not on an operational design basis. At about 150 mA, the coolant wall temperature will be about 170°C, a value beyond the saturation temperature of the coolant water at the prevailing pressures. This sets the limit for PS2 operation to be about 150-160 mA stored beam current with undulator A at a gap of 11 mm.

Photon shutter 1, with its longer mesh length and, thus, much higher pressure drop, will incur boiling of the coolant even at lower stored beam currents. Fortunately, PS1 operational requirements do not demand prolonged exposure to the undulator power densities.

The need for further research into designing FE components that can handle undulator beams with currents higher than 150 mA is critical and will be the focus during the next few years.

Commissioning Filter and Window Assembly for the APS ID Beamlines

Although the APS undulator FEs are designed for windowless operation, a special window assembly is used during the commissioning phase of the beamlines until sufficient operational experience is gained with the powerful beam from undulator A. This assembly is called a "commissioning window." Due to the high total power and power density, the filter/window assembly was designed to guarantee longevity and good performance (Kuzay et al., 1996; Shu & Kuzay, 1996). A schematic of the commissioning window is shown in Fig. 4.25. It consists of a 300-µm-thick filter block (made of graphite), a water-cooled fixed mask (made of Glidcop), a multifunctional diamond disk (made of 160-µm-thick chemical vapor deposition [CVD] diamond), and a set of windows (made of 250-µm-thick beryllium). The four blocks of the assembly, which are individually water cooled, are made to be discrete blocks aligned and fastened together instead of an integrated unit. This will allow separation of the fixed mask with its CVD diamond disk so that it can be eventually used on FEs in a windowless configuration with a differential pump. The CVD diamond disk is 160 µm thick and 25 mm in diameter and works as power filter to protect the Be window. It can also act as a contamination barrier to stop backstreaming of heavy hydrocarbons upstream from the beamline side if used in conjunction with the windowless configuration.

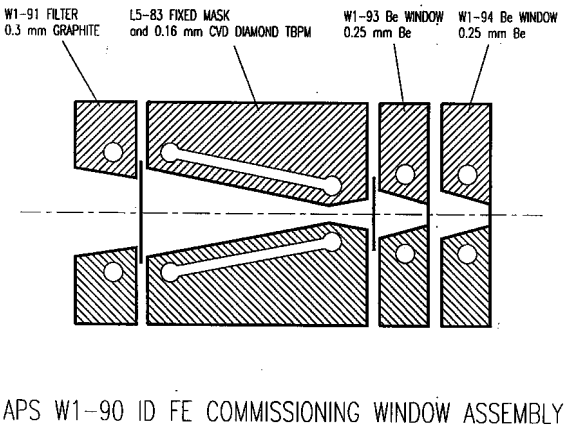

Fig. 4.25 Schematic of the commissioning window assembly for ID beamlines

For the users, the beam throughput of the commissioning window is of utmost interest. Photon transmission calculations indicate excellent transmission of radiation above about 6 keV.

Although, the commissioning windows are currently used on many undulator beamlines, only a limited amount of detailed testing has been performed. The studies have focused on the temperature measurements at the graphite filter and diamond disk with an infrared (IR) camera. These measurements are done at different undulator gaps and different stored particle beam currents. The measurements have been compared in detail with the analytical predictions. In Table 4.2, a measured set has been compared with calculations using different values for effective thermal conductivity.

It is seen from the table that agreement between the measured and predicted values is rather good. However measurements taken the same way about six months later showed much higher temperatures. At closed gap and 98 mA, a surface temperature higher than 1400°C was indicated by the IR camera. The pyrolitic graphite filter was subsequently removed and examined under microscope, which revealed a number of planar cracks in the filter around the beam footprint area that could reduce the conductive heat transfer process. Further investigations are planned in the coming year.

X-ray Beam Position Monitors

The design of the x-ray beam position monitors (XBPMs) at a third-generation synchrotron source is quite challenging. They must withstand the high thermal load (up to 600 watts/mm^2) and be able to achieve submicron spatial resolution while maintaining their stability. Both analytical and experimental results proved that CVD diamond is a good choice for the APS high heat load XBPM blade material because of its superior thermophysical properties, such as high thermal conductivity, low thermal expansion

Table 4.2 Highly Oriented Pyrolitic Graphite Filter Temperature Data Measured for Various Undulator Gaps and Stored Beam Currents (The measurements are compared with the calculations.)

Undulator Gap (mm)	Stored Current mA	Calculated Temperature in °C (effective conductivity in W/mK)	Measured Temperature in °C
11.2	92.4	792 (2.1)	785
12	94.1	776 (2.0)	779
13	94.6	695 (2.1) / 715 (2.0)	702
14	95.2	605 (2.25)	605
15	95.7	550 (2.1)	545
16	96.3	463 (2.25)	468
17	96.8	400 (2.25)	400
18	97.4	346 (2.25)	337
20	97.7		233

coefficient, and good mechanical strength and stiffness under heating. Since 1991, an extensive metal-coated CVD-diamond-based XBPM program has been continuing at the APS (Shu et al., 1992b; Shu et al., 1994; Shu & Kuzay, 1996; Patent Nos. 5,387,795 & 5,404,014).

At the APS, each beamline FE has two photoemission-type XBPMs to monitor the x-ray beam position and the angle (Kuzay, 1993; Shu & Kuzay, 1994). For an undulator FE, the present XBPM head assembly design is shown schematically in Fig. 4.26a. The first XBPM has four CVD diamond blades placed vertically in pairs. The downstream XBPM has four blades also, however, here both the vertical and horizontal blades are placed singly, and the horizontal blades are slightly tilted (Fig. 4.26b). This configuration eliminates the blade shadowing problem and somewhat mitigates the contamination of the second XBPM horizontal signal from the BM radiation. In the BM FEs, the XBPM is much simpler, consisting of only two vertical blades. A complete XBPM assembly comprises three parts, the mounting post, the stage assembly, and the blade head assembly. The error sum from these parts should meet the total error budget of $< \pm 1$ μm in position and $<\pm 0.14$ mrad in the angle of the particle beam. Both the first and second XBPM are located upstream of the user photon shutter (PS2), so they are functional whether the user shutter is open or closed (Kuzay, 1993).

The XBPM monitor has the capability to apply a bias voltage. However, the test results show that a zero bias is acceptable and has the advantage of reducing the thermal resistance caused by the bias insulator. The geometrical configuration of the APS XBPM provides a low noise environment for photoelectron current output. The XBPM was sensitive

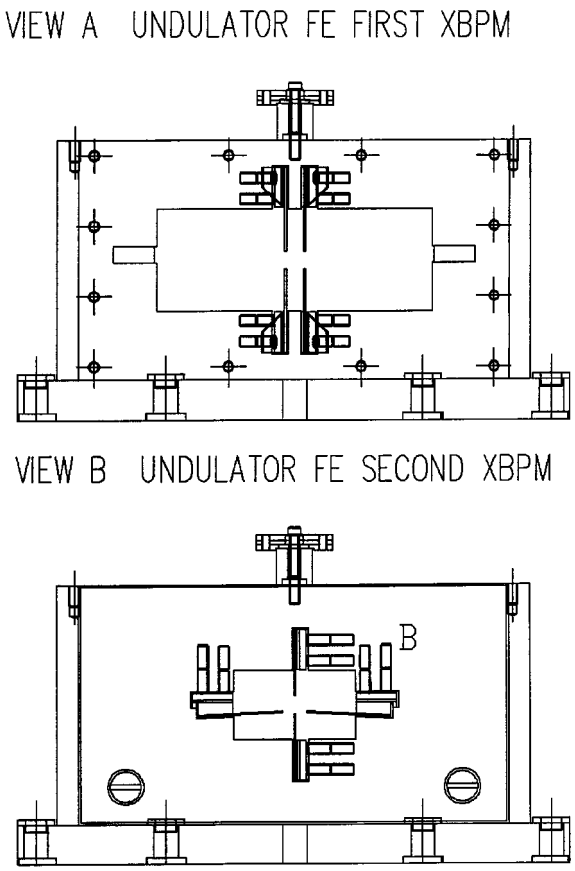

Fig. 4.26 Schematic of the XBPM head assemblies for undulator FEs, (a) first XBPM (b) second XBPM

enough to read out the photoemission signal (about 0.6 nA) from a BM source while the APS storage ring had only a 24 μA electron beam stored (during early commissioning of the storage ring in 1995). The major advantage of the XBPM is its high positioning sensitivity. Also, compared to the particle-beam position monitors in the storage ring, the FE XBPMs have much higher sensitivity to the x-ray beam angular motion simply because they are located farther from the source

The stability of the XBPM support and the motion stages is an important consideration in the overall error budget for the XBPM. The

XBPM main assembly is supported by a precision stage atop a mounting post. The post is a steel tube, filled with sand, and thermally insulated on the outside by ceramic cloth. This post design is very resilient to short-term temperature fluctuations (Kuzay, 1993). The XBPM stage assembly consists of stepping-motor-driven vertical, horizontal, and rotational stages. Because the commercially available vertical stages could not meet our specifications, we developed an in-house stage assembly. Test measurements using a laser Doppler displacement meter (LDDM) proved that the vertical stage attained a resolution of <0.2 μm with 1 μm repeatability under a 200 lb load (Barraza et al., 1994). Preliminary *in situ* vibration tests show that the XBPM main assembly maintains less than 0.1 μm rms vibration displacement level with the cooling water on.

The optimized geometric design for the blades helped reduce the BM contamination. For instance, on the first XBPM on the APS 1-ID FE, the BM contamination has been determined to be about 10% of the signal from the 2.4 m undulator A with a 15.8 mm magnet gap. Work at other synchrotron radiation sources has shown that contamination signals caused by the BM-emitted radiation is a major problem (Mulhaupt, 1995; Warwick et al., 1995). Problems are exacerbated for the XBPM when the undulators operate with different gaps, because the percentage level of the contamination will be variable. The regular XBPM calibration process can only provide signal correction for one set of conditions. During normal operations, the IDs function at varying storage ring currents, particle orbits, and undulator gaps. To offset the XBPM sensitivity to such operational variables, a newer XBPM system has been designed and a prototype built and tested for the APS.

Smart Photon Beam Position Monitor

This new XBPM system has an intelligent signal processor, which provides a self-calibration function to serve as a noise and contamination signal rejecter to improve the system sensitivity and reliability (Shu & Kuzay, 1996).

The new XBPM system configuration includes:

- a pair of photoelectron emission-style beam position monitors using CVD diamond blades for undulator beamline FEs
- a set of photoelectron current preamplifiers
- a preamplifier auto-ranging controller and digitizer
- a digital signal processor (DSP) with EEPROM database and ID source setup input interface for normalization
- a system controller with motor driver and encoder interface for XBPM calibration processes

This new system, the so-called smart photon beam position monitor (SBPM), has a built in EEPROM memory that is large enough to "remember" a complete calibration database covering all of the possible operating conditions. During the calibration mode, the monitor system controller initializes a series of automatic scan motions for the XBPM with

different ID setup information and records them into the EEPROM database array. With the XBPM operating, the system corrects the normalized output according to the undulator setup information and the calibration database. So that, with this novel system, the XBPM is always calibrated.

The heart of the smart system is a DSP TMS320c40 from Texas Instruments, Inc., which is a floating-point processor designed specifically for digital parallel processing and real-time embedded applications.

As a part of the SBPM system, a high performance preamplifier with an intelligent controller and digitizer has been designed and manufactured.

The analog part of the system is a modular, multichannel current preamplifier developed with ITHACO. The 19" rack chassis accommodates eight preamplifier channels; the ninth slot is for the APS-designed Z-180 microprocessor-based controller/digitizer. The preamplifier with controller has self-calibration and auto-ranging capabilities. The 24-bit parallel digital output includes a 16-bit A/D signal with a 10 μs conversion time and 8-bit data transform information, such as amplifier gain selection, channel word and end of conversion. The preamplifier system provides 10^4 V/A to 10^{10} V/A auto-ranging gain control in decade steps and a DC 300 Hz bandwidth.

Recent additions to the above electronics are a DSP and a system controller interface (SCI) to include an EEPROM chip, a central processing unit (CPU), and D/A converter. The SCI receives the data on the ring current, ID magnet gap, and the ID source characteristics. The normalized data from the XBPM are written on the EEPROM in a series of rapidly scanned calibration runs. (See Fig. 4.27 for a schematic of the smart XBPM electronics.) Therefore a good data bank is created in the EEPROM for the correct beam center at varying gap, current, and undulator characteristics. This allows the XBPM to have memory for changing conditions. Currently we have an SBPM installed on SRI-CAT Sectors 1, 2, and 3. However only the one on the 1-ID FE has been thoroughly calibrated to date. The other two are expected to be fully calibrated by this summer.

The most recent data for beam position and beam angle from the ID FE XBPMs with and without the DSP correction are summarized in Table 4.3. All data were taken on the 1-ID FE as the undulator A gap was varied from 11 mm to 30 mm.

An examination of the data in the table shows that the DSP correction has improved very significantly the apparent x-ray position measured by the XBPMs as the undulator gap is varied from 11 mm to 30 mm. As for the beam angle, the vertical angle indication of 280 microradians was reduced to a few microradians with the DSP corrections. The horizontal angle indication of a total of 600 microradians was also reduced to nearly zero. These are dramatic improvements and prove the power and the utility of the smart XBPM.

Further improvements in this system are needed if the signals from XBPM are to be used in the feedback system of the storage ring. This work will be continued in the coming year, while DSPs will be implemented on the beamlines in operation.

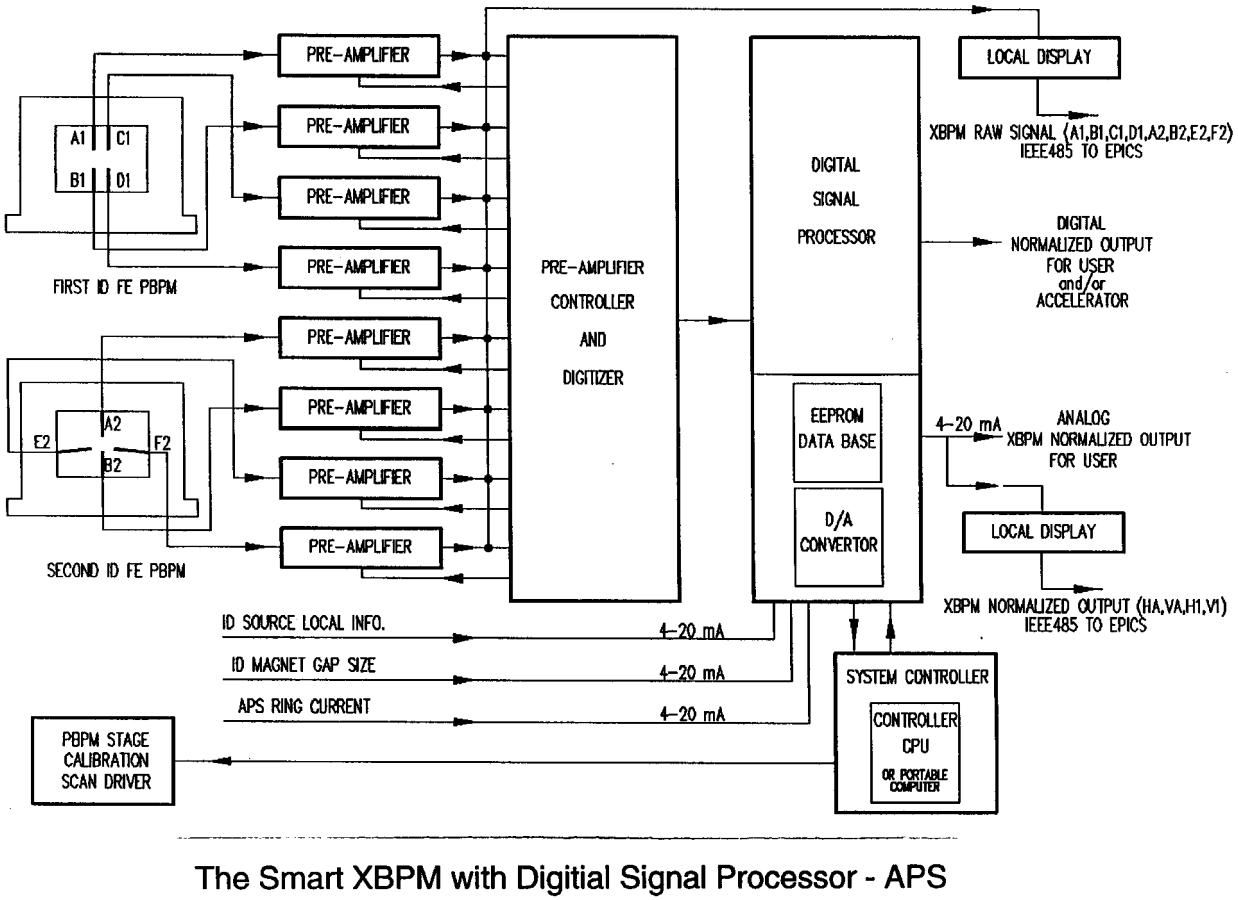

Fig. 4.27 Schematic of the electronics for the smart XBPM

Table 4.3 Improvements Obtained with DSP in XBPM Calibrations (all data taken on I-ID). Apparent x-ray beam position and angle measurements, with and without DSP, for varying undulator gaps from 11 mm to 30 mm (the actual positron beam being stable).

	Calibration Δ in position		Calibration Δ in angle	
	vertical (μm)	horizontal (μm)	vertical (μrad)	horizontal (μrad)
XPBM1	1300	100		
With DSP	12	30		
XBPM2	325	2400		
With DSP	19	42		
Without DSP			275	600
With DSP			6	8

Transmitting XBPM integrated with beamline windows

It would be useful if the synchrotron beamline window could also provide the information on the position of the beam. With this in mind, a transmitting x-ray beam position monitor was designed. The advantages of such a window will be numerous for commissioning the storage ring, FE, and beamline instruments.

In these initial studies, such a device was incorporated in the commissioning window. A CVD diamond filter, which is a 25.4-mm-diameter disk mounted on the downstream side of a fixed mask (FM3), was also designed as a transmitting x-ray beam position

monitor (TBPM) (Shu & Kuzay, 1994). The monitor blade of the TBPM is mounted perpendicular to the x-ray beam, and the blade with its low-Z metal coating is designed so that most of the x-ray beam is transmitted through the blade (Warwick et al., 1995). In this design, the 160-μm-thick CVD-diamond disk is coated in a pattern that forms four electronically isolated aluminum quadrants. The thickness of the aluminum coating is about 0.2 μm. The photoelectron emission signal is collected by a terminal interface disk, which is made from thin alumina and is coated with silver. This design concept provides the possibility of integrating the filter with TBPM functions. The beam position measurements made with a prototype of TBPM included in the commissioning window have been very instructive; the TBPM provides diagnostics capabilities during the FE commissioning, steering of particle beam orbit in the storage ring, and smart XBPM calibration. Further work will be carried out during the coming year to fully develop the system.

White-Beam Slits for ID Beamlines

Most of the ID beamlines contain a set of white-beam slits upstream of the first optical element. The major challenges in designing the white-beam slits for an ID beamline are the following:

- ability to handle high heat flux from the undulator or wiggler beam
- high precision and geometric stability requirements
- minimization of the downstream scattered x-rays
- minimization of the slit-edge fuzziness for hard x-rays

To meet these challenging design requirements, several different types of grazing-incidence knife-edge slit assemblies have been designed and manufactured. A knife-edge slit has minimum downstream x-ray scattering if the normal incident surface of the slit blade is facing the beam (see Fig. 4.28). Unfortunately, it is very difficult to design such a simple slit block because of the thermal load and high heat flux on the slit from the ID beam. To solve this problem, we turned the slit front surface around the Y axis (in Fig. 4.28) by an angle so that the x-ray beam will impinge on the slit front surface with a grazing incident angle θ as shown in Fig. 4.29. To keep the same real recess angle α, the grazing-incidence knife-edge block will have a back-cutting angle β such that:

$$\tan \alpha = \ln (1/1000)/\mu.$$

It is important to study the knife-edge fuzziness for a hard x-ray slit to determine an optimized real recess angle. If we define the ratio of output to input photon flux I/I_0 equal

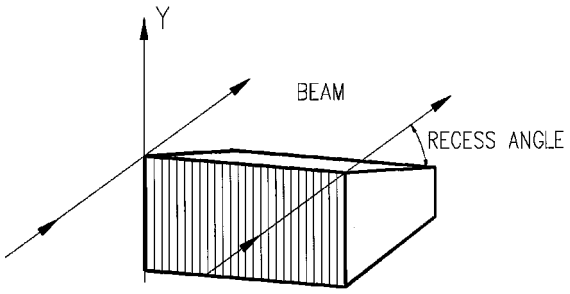

Fig. 4.28 Schematic of slit blade facing the beam

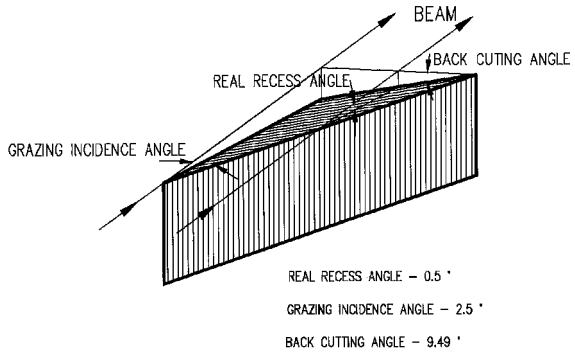

Fig. 4.29 Rotated slit blade so x-ray beam impinges on the slit front surface

to or less than 0.001 as the edge of the slit fuzzy area, we will have:

$$t = \ln(1/1000)/\mu$$

$$\text{and, } w = t \times \tan\alpha,$$

where α is the real recess angle, t is the depth to stop the beam (to 1/1000), and w is the knife-edge fuzziness (1/1000 definition).

Table 4.4 summarizes some characteristics of the white-beam slits designed and built for the APS user beamlines. All these slits have been installed on various SRI-CAT beamlines. Although initial indications are such that they may have met specifications, more quantitative data will be obtained during the coming year.

Integral Shutters

An integral shutter is a device that integrates a white-beam stop, monochromatic-beam (mono-beam) shutters, a safety stop, and a collimator into one assembly to save space and to contribute to a fail-safe personnel protection system. The major function of this shutter is to deliver either the white-radiation beam or a monochromatic beam, as desired by the user, and it is usually located between the FOE (A) and a white-beam station (B). It is one of the more popular standard components and is found in most user beamlines at the APS. The integral shutters are designed to operate in white-beam mode or mono-beam mode (Chang et al., 1995), as shown schematically in Fig. 4.30. In the mono-beam mode, the double-crystal monochromator (DCM) diffracts the beam, which is then transported to a B station. If somehow the DCM fails, the defaulted white beam is stopped by the white-beam photon shutter and the safety shutter. In the white-beam mode, the beam is transported to the B station.

Table 4.4 The Standard Slits for White-Beam ID Sources

	Source	Max. Optical Aperture	Motion Resolution	Knife Edge
L1-20	Wiggler/Undulator	48 mm (H) x 8.2 mm (V)	0.5 mm (H) x 0.2 mm (V)	Yes
L5-20	Undulator	7 mm (H) x 7 mm (V)	0.2 mm (H) x 0.2 mm (V)	Yes
L5-80	Undulator	4.5 mm (H) x 4.5 mm (V)	0.1 mm (H) x 0.1 mm (V)	Yes
L5-90	Undulator	4.5 mm (H) x 4.5 mm (V)	10 mm (H) x 10 mm (V)	No

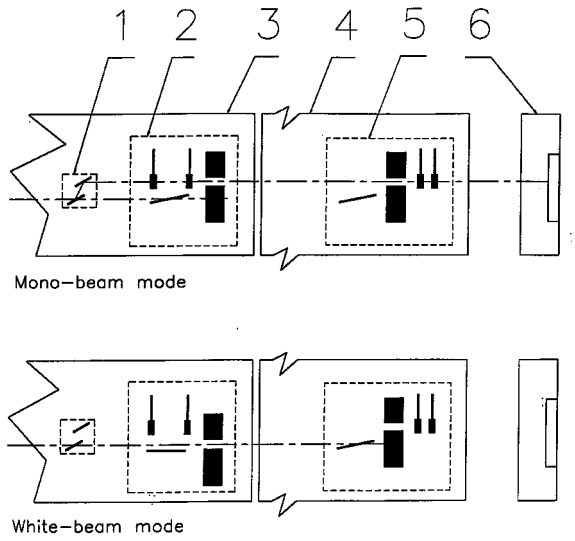

Fig. 4.30 Schematic arrangement of a typical integral shutter at the APS. (1) DCM, (2) P4, (3) FOE, (4) white-beam station, (5) P5, and (6) mono-beam hutch

Integral shutters P4 and P6 have movable stops that can stop white beam during the mono-beam mode or can allow white beam to pass during white-beam mode. Users of P4 or P6 can use either white beam or mono beam to perform their experiments. Integral shutters P5 and P7 have fixed stops that always stop the white beam and are for users who need only mono beam to conduct their experiments. Integral shutter P8 has redundant mono-beam shutters and is typically used in a mono-beam station. Integral shutter P9 has redundant pink-beam shutters, which stop both x-rays and bremsstrahlung. Other shutters with similar functions but different specifications are not discussed here.

With regard to safety, each mode of operation is secured by locking certain devices in their up or down positions by Kirk-key interlocks. The first mono-beam shutter and the second mono-beam shutter are interlocked to close simultaneously to provide redundant protection. In case of power failure or air failure, vacuum force and gravity force will close the mono-beam shutters so that they are fail-safe. There are four mechanical limit switches on each actuator to provide redundant signals for both the up and down positions for the safety interlock systems.

All the integral shutters mentioned above are operational and functional up to 100 mA operation. Of course, all the integral shutters for the BM beamlines are designed to be operated at the full power of 300 mA. All of these units have been operating with no problems. The critical element is the photon shutter, which is constructed the same way as the FE photon shutter. Because they are usually located farther downstream in the beamline, their thermo-mechanical exposure is not as severe as that for the FE shutters.

Optical Tables and Stages

Optical support systems have been successfully implemented at the APS (Barraza et al., 1994; Barraza et al., 1995; Patent No. 5,526,903). The modular designs of the positioning stages have made it possible to quickly and effectively configure different systems, including standard optical table assemblies, mirror support and positioning systems, and other custom systems designed for experiment stations. The detailed drawings and technical specifications of all these stages are available on the DX.

The performance evaluation of these systems is undertaken using a LDDM with a measurement resolution of 10 nm. As an example, the T4-54 vertical stage was evaluated for repeatability, accuracy, resolution, and straightness of trajectory. This was designed as part of a complex horizontally deflecting mirror system in which in-vacuum 5-degree-of-freedom

motions are performed externally to the vacuum chamber (Barraza et al., 1995). This stage exhibits a 10 to 12 μm accuracy error across the travel range.

Beamline Deionized Water Production/Distribution System

The high heat load components for the ID beamline FEs and various components of the beamlines use porous copper-mesh inserts in the flow channels to enhance the cooling performance in these units. The porous copper mesh is brazed into the cooling channels in most cases. It is vital that deionized (DI) cooling water, used to take the heat from such components, guard against biofouling, corrosion, and galvanic actions. As a policy, the FE DI water source cannot be used to supply cooling water to components of user beamlines in which compatible material selections for components cannot be strictly regulated. Consequently, the high heat load beamline components (white-beam slits, photon shutters of integral shutters, fixed masks in the commissioning window and on the differential pump) are supplied DI cooling water from separate, isolated systems, which are specified and maintained by the CAT.

The DI water production/distribution system was designed to support the needs of a user beamline based upon the following criteria:

- Deliver 70 gpm of DI water to the sector at 140 psi pressure
- Produce high-quality DI water (3-12 Mohm/cm)
- Operate continuously with minimal maintenance
- Be compact and able to fit through the 38 1/2" × 45 1/2" access opening into the mezzanine area where the system will be installed
- Be delivered fully assembled to minimize assembly and installation time
- Be easy to use and control

The DI water production/distribution system is compact and skid mounted, and ties into a sector's supply and return main headers for distribution to the various beamlines in the sector. A separate portable skid houses the two mixed bed resin canisters that continuously polish a slip stream of the main system flow to maintain the system water quality. The polishing loop also contains an ultraviolet sterilizer unit and ultrafine filtration to keep the water free of bacteria. Water is supplied from and returned to a large 100 gallon polyethylene tank, which houses the system heat exchanger. The water level in the tank is automatically maintained via level controls. Both the technical specifications and the servicing procedures are available from the APS DX on the Web. The system is now used by most of the CATs.

Bonding and Material Studies

An important research area that has a major impact on many of the designed components is related to bonding, brazing and welding techniques to join a variety of materials including composites. The required equipment includes ovens, quick-heat-up quick-quench vacuum furnaces for general purpose brazing (see Fig. 4.31), chemical hoods for etching, cleaning and surface preparation, microscopy,

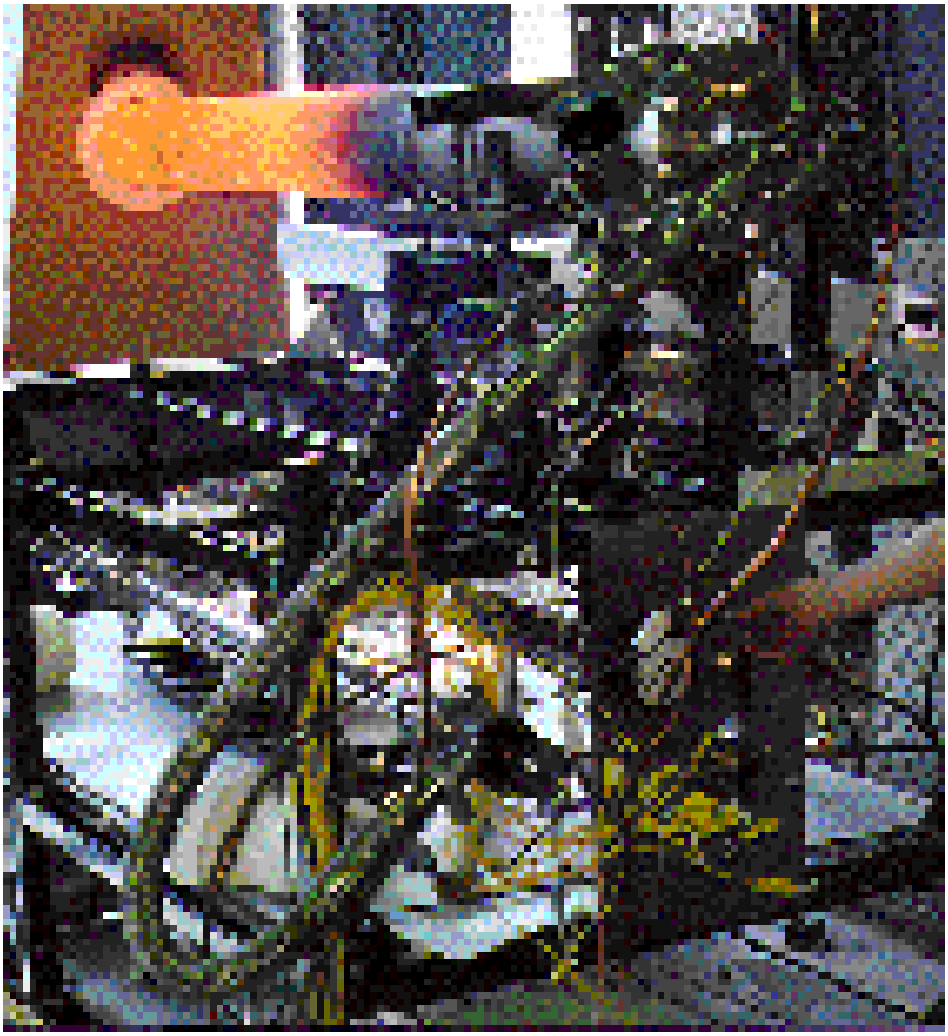

Fig. 4.31 The fast vacuum furnace heating and cooling facility is unique in the world. It is specially designed for components with high aspect ratio geometry, which is typical for high heat load components associated with large synchrotrons and third-generation light sources.

polishing and imaging facilities for metallographic and metallurgical studies. Unique expertise has been developed in the areas of Glidcop and tungsten bonding. Some of the fixed masks and photon shutters made out of Glidcop, and the tungsten slits have been brazed/bonded using these facilities. Unique capabilities developed in brazing Glidcop to Glidcop, Glidcop to OFHC copper, and Glidcop to stainless steel constitute an alternative to explosive bonding. These capabilities have benefited ASD, APS users, vendors, and other synchrotron facilities. One case in point is the fixed masks and photon shutters fabricated for SPring-8 ID beamlines.

The photon shutters and fixed masks are the components exposed to the highest heat load. The shutters are needed to stop the beam and are fabricated from high purity, high conductivity, OFHC copper with a GlidCop plate brazed or explosion bonded to the OFHC copper. The fixed masks collimate the beam and protect downstream components and beamline piping from misaligned high energy

beams that might otherwise impinge on these surfaces (Shu et al., 1992a, 1992c). The ID fixed masks are made of GlidCop.

GlidCop is often used in applications in which the component manufacturing process uses high temperatures, such as brazing and glass-to-metal sealing. GlidCop is dispersion-strengthened OFHC copper made by powder metallurgy techniques. GlidCop AL-15 is 99.7 weight percent copper (99.3% by volume) and 0.3 weight percent aluminum oxide (0.7% by volume). GlidCop annealed for 1 hour at 600°C has a yield strength of 400 MPa (58 KSI). The yield strength of copper-zirconium annealed at 600°C is 100 MPa (15 KSI), and that of OFHC copper is less than 50 MPa (7 KSI) (Samal, 1992; Samal & Nadkarni, 1984). GlidCop has 90% the thermal conductivity of OFHC copper, retains its strength after high temperature brazing, and has tensile strengths ranging from 380 to 700 MPa.

GlidCop has a pinned, fine-grained texture, which gives it high strength and resistance to softening at high temperatures. The pinning occurs due to the Al_2O_3 submicron particles in the GlidCop. A fast-cycle vacuum braze technology has been developed to use readily available, low-cost, silver-based alloys and to fabricate complex geometries while minimizing the diffusion. A quick braze cycle also minimizes alloying and dissolution that can degrade the quality of the joint.

Copper-to-GlidCop brazing has other complications. GlidCop components are adversely affected if the temperatures are more than 20°C above the melt temperature of the braze and if the melt cycle time is more than a few minutes. Expertise in brazing GlidCop with silver-based alloys has been beneficial in many ways. Stainless steel can be brazed to GlidCop by using a thermal process similar to that of brazing mesh or porous media into GlidCop. The advantage of this is that stainless-steel vacuum flanges can be brazed to GlidCop.

A photon shutter prototype has been laser tested at a power density of more than 70 watts/mm^2 for 7,000 cycles without failure of the GlidCop braze joint (Wang et al., 1994; Kuzay, 1994).

These bonding techniques developed in-house are alternatives to explosive bonding (Shu et al., 1995) in which we have also developed significant experience and which we have used extensively in making the high heat load/high heat flux standard components used for the APS FEs and beamlines.

At the APS, several tons of UHV machinable tungsten have been used for safety shutters. This UHV grade of machinable tungsten was developed by the APS working closely with two U.S. vendors.

Machinable tungsten has been successfully brazed to copper (Liu et al., 1996). Samples have been fabricated and metallurgically examined. A special fixture was developed to braze components consisting of machinable tungsten to a copper-cooling block. This capability has also been used by APS users, and the technology has been transferred to vendors.

Porous Media Heat Transfer Studies Using Liquid Nitrogen Cooling

Copper mesh, compressed and formed into porous matrices of various shapes and sizes, is routinely used in cooling channels of components for the APS FEs and beamlines to

significantly enhance the heat transfer performance of the component. A significant amount of research has been performed at the APS over the last eight years in order to better quantify and optimize the selection of mesh porous matrix attributes (porosity, wire size, core size, bonding technique, etc.) for various water-cooled component configurations (Kuzay et al., 1991; Amir et al., 1995; Sözen & Kuzay, 1996). The use of porous mesh matrices in cryogenically cooled components, such as mirrors and silicon double-crystal monochromators, also offers significant heat-transfer enhancement capabilities that improve the stability and resolution of the optics (Kuzay, 1992; Rogers et al., 1996a; U.S. Patent No. 5,123,982). To better understand cryo-cooled heat transfer, an experimental program has been developed to investigate the heat transfer limits using conductive porous matrices with liquid nitrogen as the coolant.

Early experimental studies show considerable promise in this heat transfer technology at liquid nitrogen temperatures. Although few studies have been done to date, excellent agreement with empirical correlation and models has been shown, and the heat transfer enhancement from the use of mesh has been demonstrated. The two-phase operating regime consisting of both liquid and vapor nitrogen is of particular interest, because the heat transfer values are enhanced to a greater degree compared to single-phase values. More studies involving non-brazed, epoxied, and brazed mesh inserts will be carried out in the future. Mesh heat transfer enhancement in cryogenically cooled components is expected to provide a high level of cooling performance for synchrotron optics.

Vibration Studies

Maintaining component stability plays an important role in beamline operations at the APS and in the success of scientific experiments. Random disturbances are prevalent on the experiment hall floor from automatic machinery used in the beamline and in the storage ring, regular noise from utilities, and pedestrian traffic. The design of beamline components requires that these disturbances are not amplified to unacceptable levels. The goal of the vibration studies is to characterize the structural dynamic response of various beamline components via experimental and theoretical techniques. In particular, the primarily concern is with the vibratory motions that occur at the micrometer level and at low frequency (<20 Hz).

Various experimental and theoretical studies have been undertaken during the past year that relate to the dynamic response of a standard APS optical table assembly (Barraza et al., 1994). The optical table assembly is a complex system comprising precision positioning stages and spherical bearings. The stiffness and damping properties of the flexibly suspended breadboard were estimated experimentally using modal analysis. The results show good vibration performance; the breadboard may be approximated as a rigid body when included in the theoretical analysis of the complete optical table assembly. Detailed stiffness studies for the linkages at the vertical stages were done by Basdogan and others (1996). Theoretical and experimental studies for the estimation of the damping and stiffness properties of the vertical stages are still in progress.

Research is ongoing to improve submicron vibration measurements on systems that are of smaller mass. This issue is critical in the selection of sensors, because, in some cases, the choice of sensor may alter the inertial properties of the system under evaluation. Therefore, a noncontact approach is more suitable. Currently, a 10-nm-resolution LDDM is being used for measuring fine motions and is under development for use in low frequency vibration measurements of these smaller mass systems.

4.2.3 Summary of Future R&D Activities

During the coming years, the Beamline Engineering Group will be looking into a variety of R&D issues in support of users' needs for their beamline operations. The major ones are:

- SPring-8 FE component R&D (see Chapter 5)
- Bonding and material studies
- DSP for the smart XBPM application
- Sub-nanoradian angular decoder development (with LDRD support)
- Cryo-cooling heat transfer
- Vibration studies on mirror tank mounts
- Mechanical design for a UHV monochromator
- Intelligent user filters that use fuzzy logic
- Sector 4 beamline design for SRI-CAT
- Position sensitive photoconductive detector (PSPCD) development (with LDRD support)

4.3 High Heat Load X-ray Optics

4.3.1 Introduction

The issue of thermal management in optical components (mirrors and single-crystal monochromators) is one of the most challenging technical problems associated with the third-generation of hard x-ray synchrotron sources. Undulators placed on the straight sections of the APS storage ring can produce a total power in excess of 5 kilowatts and power densities in excess of 160 watts/mm^2 at a typical source-to-first-optic distance of 30 meters with 100 mA of stored beam. It is the job of the optics designer to develop components that can operate efficiently under the influence of these high heat load x-ray beams and that can deliver the x-ray beam to the experiment with the least possible loss in brilliance. Among other things, this means that the thermally induced slope errors must be reduced to well below the opening angle of the x-ray beam itself. The enormity of the task becomes quite evident when one considers that the radiation emitted from undulators at the APS has a vertical opening angle of only 15-20 microradians or about 3-4 arc seconds full width half maximum (FWHM).

At first, the problem may seem simply one of removing heat absorbed in the optics; however, removal of the deposited power is only one ingredient in the larger challenge of